

Characterizing the Skin Microbiota in *Rana catesbeiana* Across Natural Metamorphosis and Hormone Exposure

This manuscript ([permalink](#)) was automatically generated from [imasianxd/ProjectFrog_MANUSCRIPT@e386527](#) on June 14, 2021.

Authors

- **Jacob Imbery***

University of Victoria, Victoria, BC, Canada

- **Baofeng Jia***

 [0000-0002-4735-4709](#) ·  [imasianxd](#) ·  [bfjia](#)

Department of Molecular Biology and Biochemistry, Simon Fraser University

- **Thea Van Rossum**

Department of Molecular Biology and Biochemistry, Simon Fraser University

- **Caren C. Helbing**

University of Victoria, Victoria, BC, Canada

- **Fiona S.L. Brinkman**

 [0000-0002-0584-4099](#)

Department of Molecular Biology and Biochemistry, Simon Fraser University

Abstract

Municipal wastewater is one of the principal sources of contaminants delivered into urban aquatic environments. These contaminants include endocrine disrupting compounds (EDCs), which can perturb diverse biological processes by disrupting normal endocrine functions even at the levels found in treated wastewater effluents. Current wastewater regulations, testing methodologies and management strategies often do not take EDCs into account, further, even when testing strategies are in place, EDCs are often biologically active below detection thresholds. The effect of EDCs is seen in a North American Xenopus (bullfrog) metamorphosis model, where transformation of an aquatic tadpole into a juvenile frog can be disrupted by their presence. Although there is the potential to use amphibian metamorphosis as an assay for EDC presence, current methodologies rely on a 21-day morphological assessment. However, the use of microbiome profiling is quickly emerging as a novel tool for understanding environmental toxicants and their impact with a lower detection threshold than current chemical tests. Here, we used 16S rRNA sequencing to profile the skin microbiome of the bullfrog at different developmental stages as well as upon exposure to thyroid hormones T3 and T4 to investigate if the bullfrog skin microbiome can be used as an indicator of environmental EDC contamination. We found that bacterial communities on the frog's skin shifts as they develop from tadpoles to froglets. This is characterized by a significantly reduction in alpha diversity and increased abundance of a Verrucomicrobia sp. in froglets than found on younger frogs. However, neither acute T3 or T4 exposure had a significant effect on the tadpole's skin microbiomes. These results suggest

that acute hormone exposure via ECD-contaminated waste water can have minimal direct effects on the *Lithobates catesbeianus* skin microbiome. Taken together with the differences observed in the microbiome with metamorphic stage, the skin microbiome is predominantly determined by the host animal. This suggests that the skin microbiome may be a suitable tool to monitor EDCs at levels that are biologically consequential without a tendency for false positives.

Keywords

Microbiome, Hormone Exposure, Development.

Introduction

Bullfrog developmental models are very sensitive to exogenous T3, as well as their sex ratios are affected by endocrine disruption in the environment. Therefore bullfrogs' skin can act as a sensitive model to study effects of hormones and disruptors on the environment. Frog metamorphosis represents the most accessible and striking example of TH action. This process is entirely dependent upon TH and completion of this developmental period requires a rise in TH levels from zero baseline levels found in the premetamorphic tadpole. TH levels naturally increase from premetamorphosis through prometamorphosis to reach maximal levels at metamorphic climax at which time rapid, overt remodeling of the tadpole into a froglet occurs. Virtually all tissues are targets for TH action, yet the end result includes diverse responses e.g. complete tail resorption, liver reprogramming, brain remodeling, and limb growth. These changes are precociously induced in the premetamorphic tadpole by exogenous administration of T3 or T4

Our frog species, Ranidae frogs The current OECD 21 day assay evaluates the whole organismal response with assessment of external morphological criteria at days 7 and 21 and qualitative assessment of thyroid gland morphology at day 21. It relies upon highly inbred laboratory strains of *Xenopus* species that are not relevant to the North American environment.

Previous work used RNA-Seq and Kraken filtering to demonstrate that Ranavirus infection resulted in a differential abundance of bacterial transcripts from specific bacterial communities. I have applied the same Kraken filtering techniques to RNA-Seq datasets from tail fin (TF) and olfactory epithelium (OE) tissues from pre-metamorphic bullfrog tadpoles exposed to either E2, T4, or T3. This data will be paired with traditional 16S rRNA sequencing methods to examine the effects these exposures have on the *Rana catesbeiana* bacterial and viral communities.

The skin microbiome of land and marine animals contains highly diverse microbial communities that is characteristic of it's host [1]. As microbiome studies become popular, research had shown that the skin micobiota changes between host life stages, environmental conditions, health state, and geographical locations [2,3,4]. Often, the skin is the first barrier to contaminants and support antagonistic effects against stressors [5,6,7]. While the skin microbiome of marine and land mammals has been of interest recent years [8], very little is known about the skin microbiota of amphibians, especially the effects of natural metamorphosis on their skin microbiota. Given the successful identification of microbiome biomarkers in human, animal, and environmental settings [9,10,11], the skin microbiome of tadpoles and frogs may represents an innovative biomarker approach to monitor environmental contaminants exposure

This work is part of the WEC project in which the response of pre-metamorphic tadpoles is measured to 3 different hormone treatments: Thyroxine (T4), triiodothyronine (T3), and 17-beta-estradiol (E2). T4 is the precursor to the more bioactive thyroid hormone, T3. E2 here, acts a control group for hormone

exposure, but is also used to monitor potential crosstalk between thyroid- and estrogen-mediated pathways.

Methods

Sampling

Premetamorphic tadpoles (TK stages I-VI) were exposed at 21 °C for 48 h to concentrations of T3 (Sigma-Aldrich, Oakville, ON; Catalog #T2752, CAS 55-06-1), T4 (Sigma, Catalog #T2501, CAS 6106-07-6), or E2 (Sigma, Catalog #E4389, PubChem Substance ID: 329799056). Five tadpoles per exposure condition were exposed to either 10 nM T3 in 40nM NaOH, 50 nM T4 in 50nM NaOH exposure, 10 nM E2 in dechlorinated water, or their respective vehicle control. The concentrations chosen were based upon observed physiological and environmental relevance [??? et al., 2016] After completion of the experimental exposures, tadpoles were euthanized in 0.1% buffered tricaine methanesulfonate (TMS, Aqua Life, Syndel Laboratories, Nanaimo, BC, Canada) and the TF and rostrum were dissected, preserved in RNAlater solution (Ambion, Foster City, CA, USA), and stored at -20 °C. The rostrum was halved and sub-dessected to isolate the olfactory sac containing the OE. The OE and TF from each sample animal were then combined in 300 µL TRIzol and mechanically disrupted in a Retsch MM301 Mixer Mill (Thermo Fisher Scientific, Ottawa, Canada) at 25 Hz for two 3-min intervals, separated by a 180° rotation of the samples. After pelleting insoluble material with centrifugation at 12,000 ×g for 10 min at 4 °C, the supernatant was transferred to a new RNase-free tube. RNA was extracted and washed using chloroform, isopropanol, and ethanol treatments and subsequently dissolved in 30 µL diethyl pyrocarbonate-treated water (Sigma-Aldrich) and stored at -80 °C.

16S rRNA Amplicon Sequencing

We performed 16S ribosomal RNA (rRNA) sequencing on 38 tadpole and frog samples, 5 control swabs from gloves and swabs, and 6 control swabs from tank biofilm and water. A set of positive controls consisting of predefined communities, and negative controls were also included as part of the sequencing experiment. The 16S rDNA was amplified using the following primer pair. Forward: Klin16SF: 5'-TCGTCGGCAGCGTCAGATGTGTATAAGAGACAGAYTGGGYDTAAAGNG-3' and reverse Klin16SR: 5'-GTCTCGTGGGCTCGGAGATGTGTATAAGAGACAGTACNVGGGTATCTAATCC-3' After amplification, the amplicons are prepared for sequencing following the Illumina 16S Metagenomic Sequencing Library Preparation guide (Ref. Illumina. 2017). The success of library preparation was verified by agarose gels. Equimolar amount of all samples with an additional positive and negative control was pooled and sequenced in four independent runs with the Illumina MiSeq platform using the MiSeq Reagent Kit V2 (Illumina), producing 251 bases paired end reads. The sequence data is available in NCBI SRA database under biosample ID 123456789.

16S rRNA Amplicon Analysis

Raw sequencing reads were demultiplexed and processing within QIIME2 (Ver. 2018.4) [12] following the standard ASV identification workflow. Amplicon sequence variants (ASVs) identified using QIIME2 submodule DADA2 [13]. Taxonomic assignment of ASVs was done using QIIME2 VSEARCH submodule against the Silva 16s rRNA database (ver. 132, 99%); [14].

Alpha diversity of microbiomes was calculated using the Shannon-Wiener Diversity Index. Beta diversity was measured using the Bray-Curtis distance and visualized using 2 or 3 axis Non-metric Multi-dimensional Scaling (NMDS). Taxa abundance correlation with tadpole length and weight was identified using pearson correlation. The significance of differential taxa abundance between groups was calculated using Kruskal-Wallis H test followed by a pair-wise Student's t-test. False discovery rate adjusted using the Benjamin-Hochberg procedure.

Meta-transcriptomic Sequencing

The RNA quality and quantity were verified by a Nanodrop spectrophotometer (Thermo Scientific NanoDrop One spectrophotometer, Thermo Scientific). The integrity of isolated RNA was analyzed using a Bioanalyzer 2100 (Agilent Technologies), and samples with RNA integrity number (RIN) of > 7 were used for RNA-Seq analyses (5 biological replicates per treatment). RNA samples were shipped on dry ice to Canada's Michael Smith Genome Sciences Centre (GSC, BC Cancer Research, Canada), where strand-specific mRNA libraries were constructed and sequenced using Illumina HiSeq 2500 (paired-end platform generating 2 x 75 base pair reads for each sample). The sequence data is available in NCBI SRA database under biosample ID 123456789.

Meta-transcriptomic Analysis

Our RNA-Seq analysis pipeline follows the schematic presented in figure (Fig. 12). Reads quality was assessed using FastQC to ensure high read quality in all samples. Using TransAbyss, the fastq reads generated from each sample was assembled de novo into a reference transcriptome library representing each transcript that could be assembled given the paired-end reads supplied. We created a complete reference transcriptome assembled using TransAbyss. All reference transcriptome libraries were then merged and filtered to remove duplicated sequences, and this merged reference transcriptome was filtered through a large library of microbial RefSeq sequences using Kraken2 to create a library of microbial transcript sequences that were found in one or more of the sequenced samples.

Kraken2 is a taxonomic classification system that relies on exact k-mer matches instead of percent identity and coverage. Kraken2 matches the query sequences to the lowest common ancestor that is matched within the selected database. Kraken2 will assign a taxonomy if the number of identical k-mer matches passes a threshold percentage of all k-mers of a given sequence, as set by the user. The optimal threshold for taxonomic assignment in this dataset was determined to be a 40% confidence threshold of k-mer matches (Fig. 13).

The Kraken2 database used to filter for microbial transcripts includes the following RefSeq sequences:
-Archaea: RefSeq complete archaeal genomes/proteins
-Bacteria: RefSeq complete bacterial genomes/proteins
-Viral: RefSeq complete viral genomes/proteins
-Human: GRCh38 human genome/proteins
-Fungi: RefSeq complete fungal genomes/proteins
-Plant: RefSeq complete plant genomes/proteins
-Protozoa: RefSeq complete protozoan genomes/proteins

Human RefSeq sequences were included in the Kraken2 filter in order identify human contamination and separate these transcripts later in the microbial RNA-Seq pipeline.

We used this new filtered list of microbial transcripts as our microbial reference transcriptome and remapped the raw reads from each sequenced sample to this new reference using Burrow-Wheeler Alignment tool. The mapped reads were assembled into transcripts and counted for differential expression analysis using DESeq2. We then extracted two lists of sequences for each WEC exposure condition and tissue type: one list containing all transcripts that were significantly represented in the majority of samples within a given exposure and control set ($\text{cpm} > 0.1$), and one list containing all transcripts that were significantly differentially expressed with a specific exposure condition. These two lists were then fed through the kraken2 databases consisting of each of the RefSeq libraries above, which will assign a taxonomy to a transcript at a match threshold.

Results

Lithobates catesbeianus skin microbiomes is unique and distinct compared to it's environment.

A total of 341 samples, including negative controls (n=11), positive controls (n=10), swab (n=6) and glove (n=6) controls, were sequenced in four sequencing experiments. Combined, there were 56 tank biofilm microbiome samples, 79 natural metamorphosis frog microbiomes and 96 hormone exposed frog microbiomes. Across all experiments, we produced 46.7million reads assigned into 19,850 amplicon sequencing variants (ASVs). Both the negative and positive sequencing control produced taxa distributions as expected, with negative controls generally having reduced to zero number of reads compared to swabs (Fig. 1). Using NMDS and k-means clustering using bray-curtis distance measurements, the frog microbiomes are distinct from the controls and surrounding water (Fig. 2). There exist a small overlap between tank water and frog skin communities. We note that the control samples as well as some skin samples had a low number of reads.

Characterization of Lithobates catesbeianus skin bacterial microbiome across life stages.

Overall, nine phyla represented <98% of all bullfrog microbiomes (Fig. 3). Of the nine phyla, it can be classified into 25 genera that composed of >60% of the microbiomes, on average (Fig. 4). Proteobacteria, Verrucomicrobia, and Bacteroidetes were the three most abundance phyla.

In frogs that metamorphized naturally, the microbiome changes significantly with stages of development. Furthermore, the microbiomes of tadpoles and froglets are distinct from each other (Fig. 5). The abundance of Verrucomicrobia increases with developmental stage, with a remarkable 3-fold increase between froglets and tadpoles. This increase is corresponded to a significant ($q<0.01$) decrease in Bacteroidetes, Firmicutes, Fusobacteria, and most abundantly, Proteobacteria (Fig. 3, Fig. 6). The increase in Verrucomicrobia is composed of an increase in the order Verrucomicrobiales. A small proportion (<15%) of Verrumicrobiales were classified to the genus Akkermansia. However, the ASVs identified did not provide the resolution necessary for the further classification of ASVs associated with Verrucomicrobiales.

Other genera that had a >2fold increase were Tumebacillus, Duganella, Janthinobacterium, Massilia, and Novosphingobium. Of the decreasing taxa, Cellulosilyticum, Romboutsia, and Cetobacterium were the genera that exhibited a >2fold decrease in abundance. Lastly, we note a significant decrease in alpha diversity of froglets compared to tadpoles as measured by the Shannon index (Fig. 7).

By contrast, hormone exposed tadpoles did not exhibit a strong shift in their microbiomes throughout their developmental stage. Bacteroidetes, and Proteobacteria were again the dominant phyla similar to the microbiomes of tadpoles that underwent natural metamorphosis. Regardless of hormone (i.e. T3, T4, or E2), there were no significant changes in phyla composition (Fig. 8). There were also no change in alpha diversity as the tadpoles age.

The sex of the frog had no significant impact on the community composition. (Fig. 9) The weight and length of tadpoles of naturally developing, but not hormone exposed, frogs correlated with shifts in taxa abundances of the microbiomes.

The effect of E2, T3 and T4 Exposure on the Lithobates catesbeianus skin microbiome.

The skin microbiome were analysed based on samples exposed to E2, T3 or T4 across premet, and promet life stages.

No significant changes in taxa abundance identified in tadpole microbiomes exposed to the E2, T3 and T4 hormones with respect to their control. NMDS plots calculated using the Bray-Curtis distance did not produce any clustering between control and exposure conditions (Fig. 10) However, there was a significantly increased alpha diversity of T4 exposed tadpoles (Fig. 11).

Meta-transcriptomic analysis of E2, T3, and T4 Exposure

From the counts generated from the tank water data set, primarily proteobacteria and Bacteroidetes were counted, specifically bacteria from the flavobacterium genus. Assigning bacterial taxonomies to de novo assembled transcripts from the TF and OE of tadpoles from the E2, T4, and T3 exposure sets revealed the presence of mostly bacteria from the proteobacteria phylum, with a smaller portion of bacterial transcripts mapping to gram positive phyla actinobacteria and firmicutes in both tissues (table 2, table 4). The OE had more bacterial transcripts that were significantly represented compared to the TF. Agrobacterium and Pseudomonas species exhibited the most varieties of transcripts of all present species. TFT3 exposure resulted in the differential expression of T226 16S ribosomal RNA that is assigned to *Micrococcus luteus* (Table 3). The *M. luteus* transcript exhibits a 6.5-fold change in transcript abundance (table 9). The *M. luteus* transcript exhibits similarity to an *M. luteus* 16S rRNA gene (Accession MT611279). No other treatments results in differential expression of other bacterial transcripts. Viral taxonomies were also assigned to assembled transcripts. There are fewer viral transcript assignments than bacterial in both tissues (table 5, table 7). The distribution of viral families assigned transcripts is very similar between tissues, with the majority belonging to Iridoviridae, followed by Adenoviridae, and Siphoviridae. Three viral species were commonly assigned to transcripts from both tissues: proteus phage VB_PmiS-Isfahan, Frog virus 3, and human mastadenovirus C. In the TF, T4 exposure results in the differential expressed of a single transcript assigned to the Frog virus 3 species (Table 7) with a 5.5-fold change of transcript abundance (table 13). Through a blastn query, this transcript is confirmed to encode for a hypothetical protein FV3gorf78L from the Frog virus 3 genome which contains an RNA recognition motif. T3 and E2 exposure did not result in the differential expression of any viral assigned transcripts in the TF. In the OE, both T4 and T3 exposure results in the differential expression of viral assigned transcripts from Proteus phage VB_PmiS-Isfahan, however, these are annotated with the human mitochondrial genome and are likely not viral transcripts (table 14-17). No significant results were found from filtering with the other RefSeq databases with Kraken2.

Discussion

This study characterized the skin microbiome of North American *Xenopus* frogs as it metamorphosizes naturally as well as when exposed to endocrine disrupting compounds (EDCs). These data combined gave us an overview of 1) the core frog skin microbiome, 2) variations of the skin microbiome through tadpole development and metamorphosis, and 3) potential effect of EDCs on the skin microbiome through development.

The Tadpole Skin Microbiome is Unique and Shares a Core Composition that Changes With Natural Metamorphosis

Analysis of the tadpole and froglet microbiomes revealed a Proteobacteria domination in their core microbiome. However, this core composition shifts to a Verrucomicrobia dominance as the tadpoles naturally metamorphosizes to froglets. This increase in Verrucomicrobia is composed of an increase in the order Verrucomicrobiales. There was not enough resolution to classify these ASVs further. These predominant phyla found in the frog skin microbiomes are consistent with the skin microbiomes of other marine mammals in both the wild and captive (For example: Killer whales [15], captive dolphins [16]).

EDC Exposure Did Not Lead to Any Changes in the Frog's Microbiome.

The 16S sequencing results demonstrated no significant differences between the microbiomes of E2, T3 and T4 exposed tadpoles. However, the assigning of bacterial taxonomies to expressed transcripts reveals a very slight response with T3 exposure in both tissues and T4 exposure did not result in the differential expression of any bacteria-assigned transcripts (table 3, table 5).

Assigning bacterial taxonomies to assemble transcripts revealed similar bacteria phyla as the 16S sequencing result. Both techniques capture mostly bacteria belonging to the phylum proteobacteria, with firmicutes captured as well. 16S sequencing uniquely captures the presence of Bacteroidetes and fusobacteria, where RNA-Seq methods capture the presence of actinobacteria.

The microbial RNA-Seq only detected a difference in bacteria-assigned transcript response with the T3 exposure (table 3, table 5). The transcript assigned to *C. botulinum* transcript exhibits significant abundance in all exposure sets and appears to be responsive to T3 exposure in both tissues. Since the blastn annotation of this gene returns *X. laevis* rRNA as the top hits, it is unclear whether this transcript is really from a bacterial rRNA gene and has been misannotated in NCBI's database or is a frog gene and happens to have at least 40% of its k-mers being identical matches to *C. clostridium*. The transcript assigned to *M. luteus* is confirmed to be a segment of the 16S rRNA gene from that bacterial species with the blastn annotation. This bacteria is commonly found in soil, dust, water and air, and as part of the normal microbiota of the mammalian skin [17].

The microbial RNA-Seq method captured a variety of virus-assigned transcripts that cannot be captured with 16S sequencing methods (table 6, table 8). In this dataset, there is likely a high false positive from human contamination due to retroviruses in the virus database which may have gene segments that match the human genome. The presence of mostly ranavirus represented in these data supports that this method is actually capturing the presence of viral transcripts (table 7). The differential expression of the frog virus 3 annotated transcript is the most interesting result from this investigation, although there is not much information available about this gene. The transcript is confirmed to be a viral-protein encoding gene by blastn annotation and exhibits a 5.5-fold change with T3 exposure in the TF (table 13). Frog virus 3 can be commonly isolated from healthy frogs and its role in frog disease is unknown [18].

Three different transcripts assigned to Proteus phage VB_PmiS-Isfahan are differentially expressed in either the OET3 or OET4. All these transcripts exhibit a roughly 0.5-fold change with either T3 or T4 exposure and are present in quite high abundance of 600 to 1800 median counts (table 14 - 17). These transcripts are likely false positives as they are annotated to be from human mitochondrial genomes following a blastn query. A transcript assigned to Human endogenous retrovirus K is also differentially expressed in the OE, with a 3-fold change in transcript abundance with T3 exposure (table 18). This transcript is in much lower abundance and although it was determined to be the HERV-K gene from this retrovirus, it is still likely that this is a false positive from human contamination.

Acknowledgements

The authors would like to thank their funders and the Simon Fraser University (SFU) Research Computing Group and Compute Canada for compute resource support.

Funding Information

B.J. holds Canadian Institutes of Health Research (CIHR) doctoral scholarships and Simon Fraser University (SFU) Omics and Data Sciences fellowships. F.S.L.B. holds an SFU Distinguished

Professorship. Additionally, this work was partially supported by Genome Canada and NSERC grants to R.G.B. and F.S.L.B.

Conflict of Interest

The authors declare no competing interests.

References

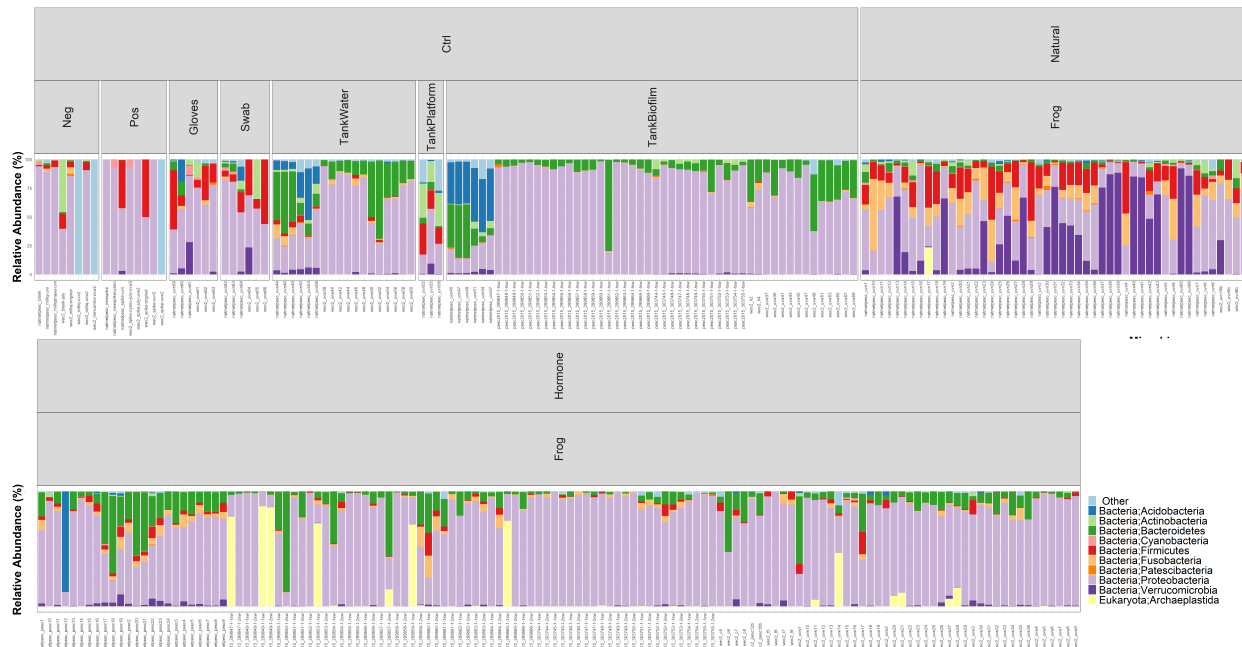


Figure 1: The relative phylum abundance of all sequenced microbiomes. X-axis represents an individual sample sorted by it's experiment set (top category) and source (bottom category). Proteobacteria is the most abundant phylum.

Clustering of Samples According to CustomGroup1

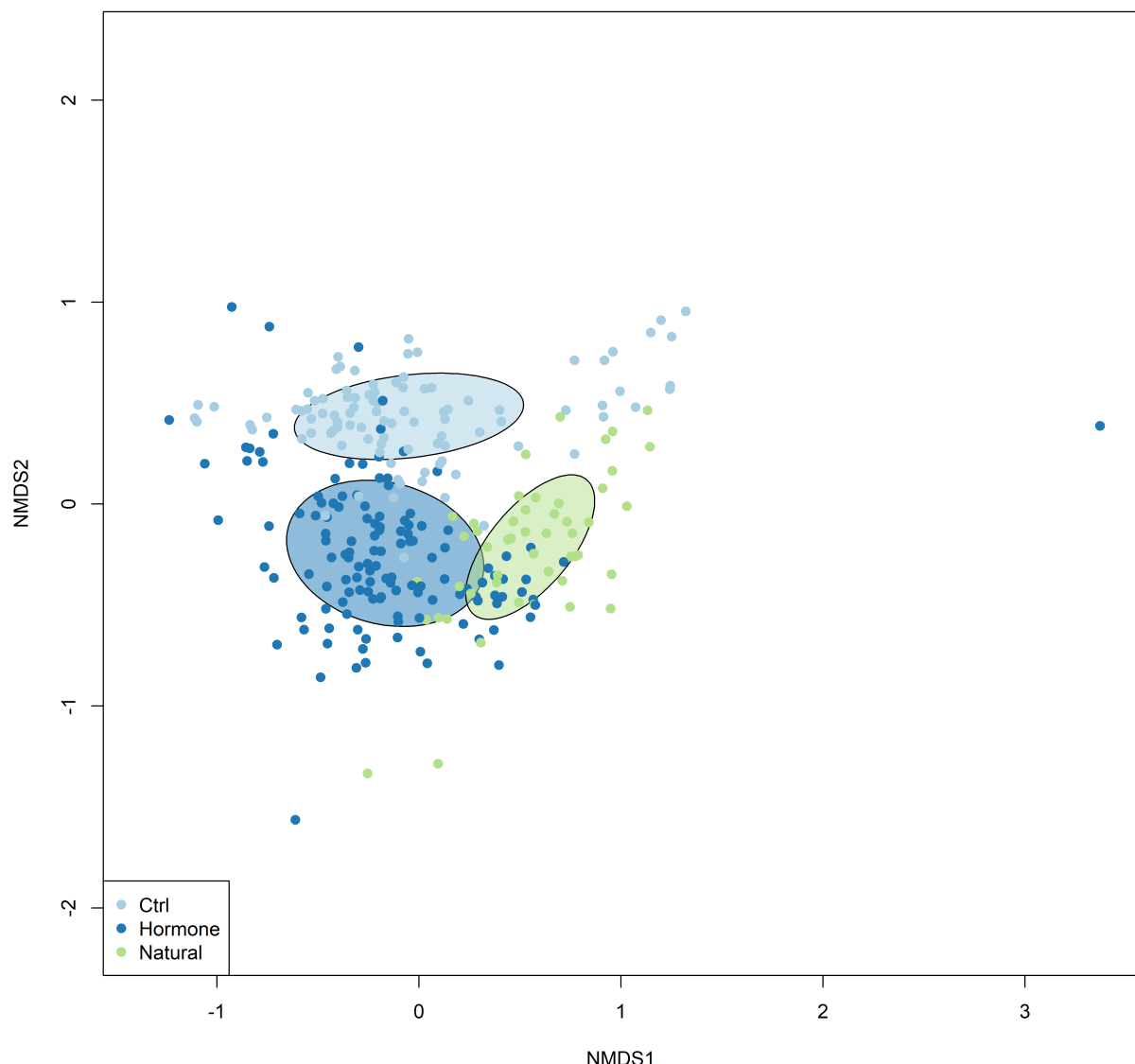


Figure 2: The tadpole and frog microbiomes are distinct and separate from controls. Using Bray-Curtis distances of the microbiomes plotted on a 2-axis NMDS, 3 distinct clusters formed, each representing a unique dataset. Both the natural metamorphosis(green) and hormone exposed (dark blue) microbiomes are distinct from the control (tank water and biofilm) microbiomes (light blue)

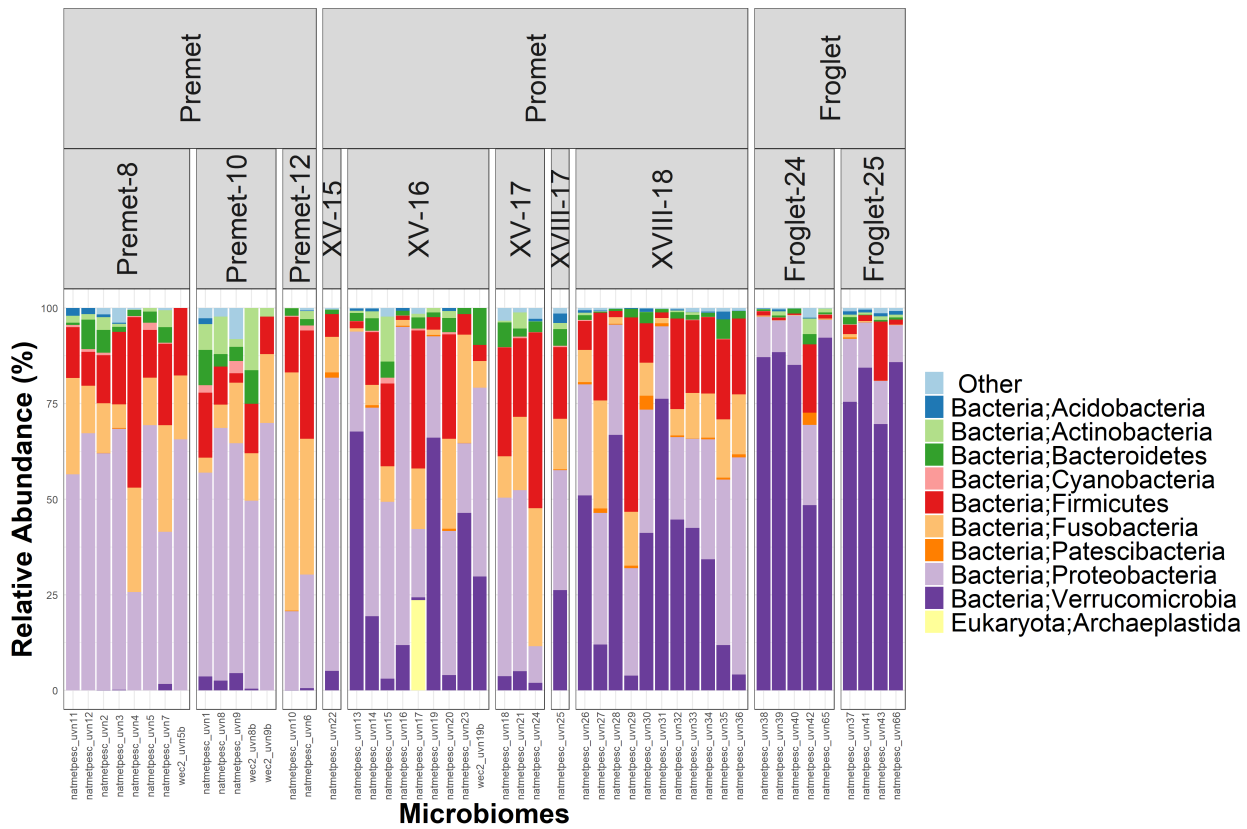


Figure 3: Relative phyla abundances of the tadpole microbiomes that underwent natural metamorphosis. The skin microbiomes (X-axis) of the tadpoles and froglets, classified according to their stage of development (bottom categories), are composed of 9 major phyla. A marked increase in Verrucomicrobia is seen as the tadpoles matures into froglets.

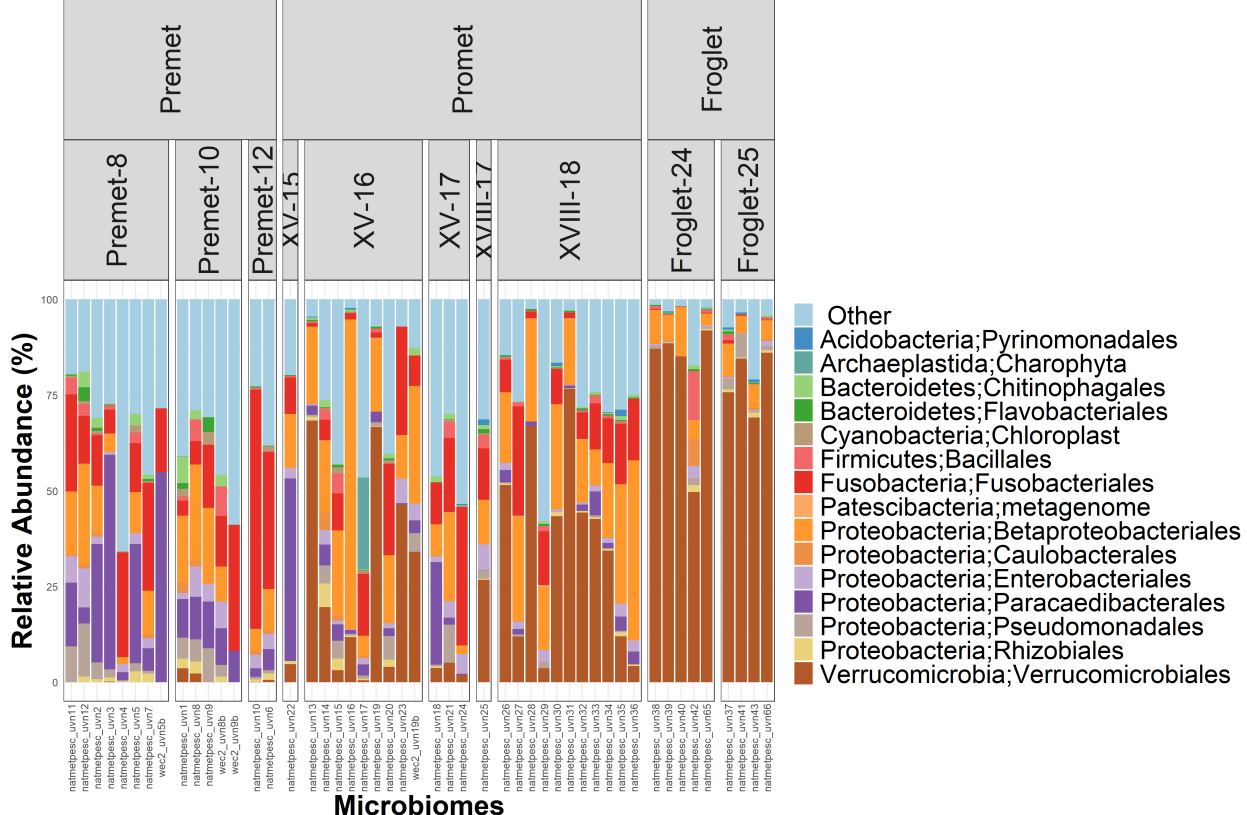


Figure 4: Relative genera abundances of the tadpole microbiomes that underwent natural metamorphosis. 25 genera made up <60% of the skin microbiomes (X-axis) of the tadpoles and froglets.

Clustering of Samples According to MetStage3

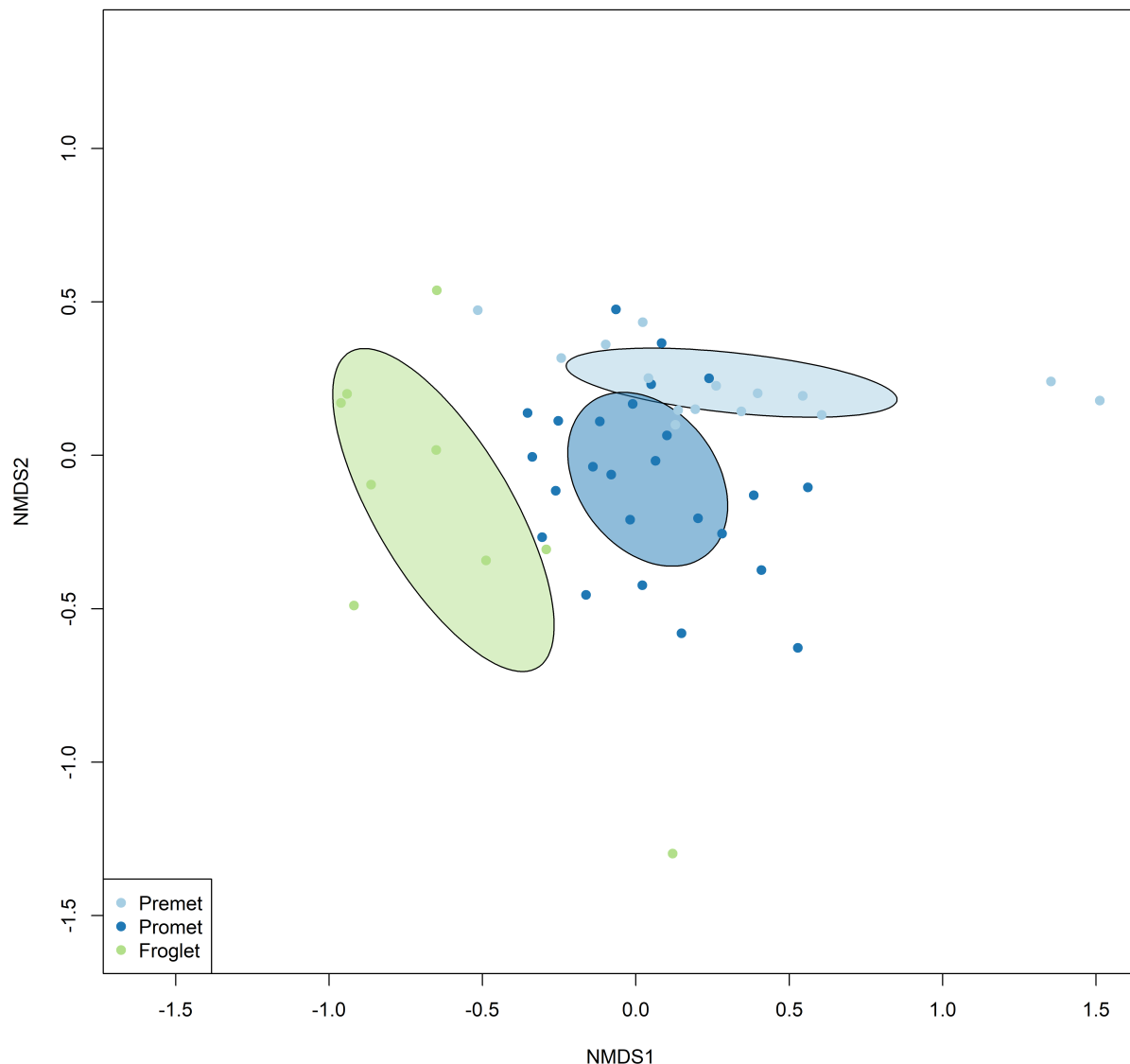


Figure 5: Clustering of microbiomes according to the frog's metamorphosis stage. The microbiomes of more developed froglets (green) are distinct compared to tadpoles (blue).

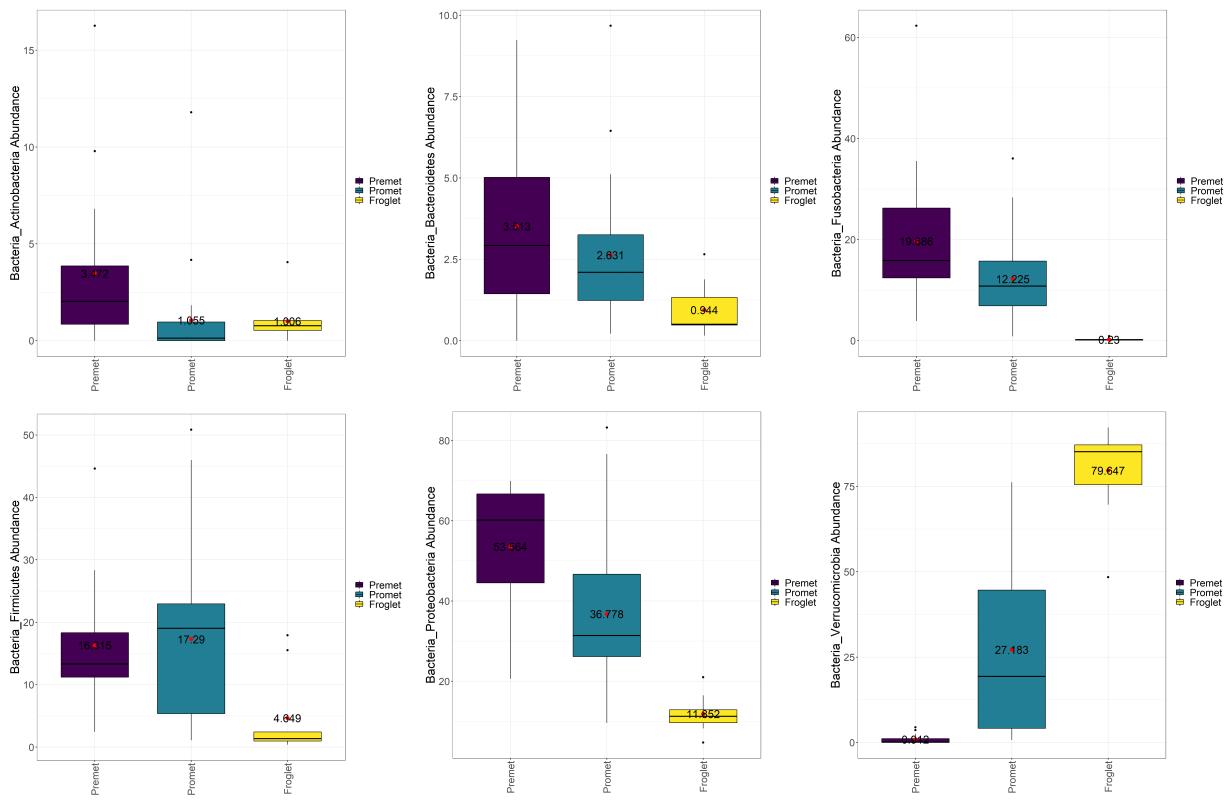


Figure 6: Differential phyla abundances between tadpoles and froglets. Four phyla had significant changes >2 fold between tadpoles (purple) and froglets (yellow) developmental stage. Bacteroidetes, Firmicutes, Fusobacteria all exhibited significant ($q<0.01$) decreases in their abundance while Verrucomicrobia increased as the tadpoles metamorphosized into froglets.

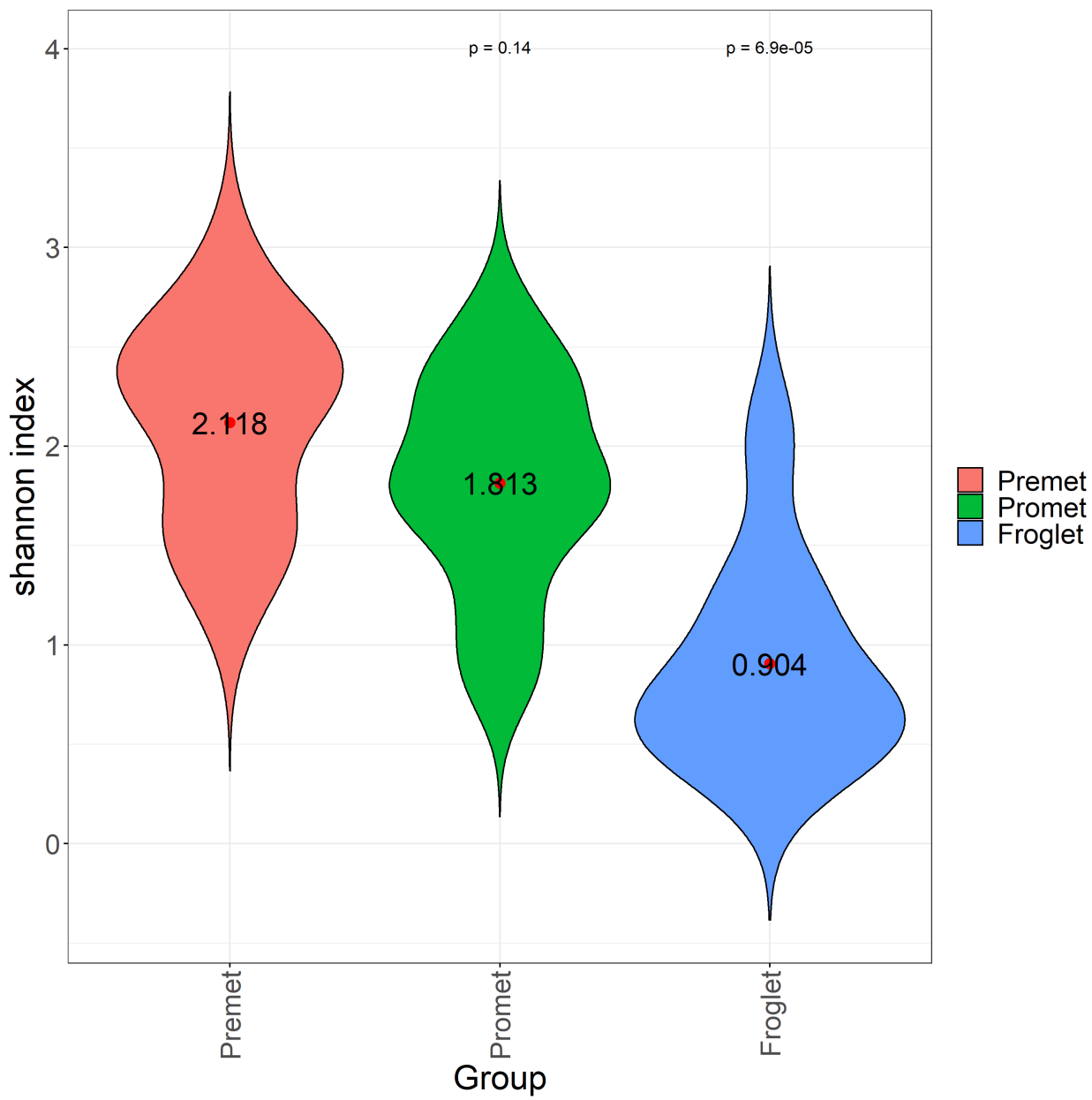


Figure 7: Alpha diversity of tadpoles are higher compared to froglets. Froglets (cyan) exhibited a significant ($q < 0.01$) decrease in alpha diversity as measured by the Shannon Index compared to tadpoles (orange).

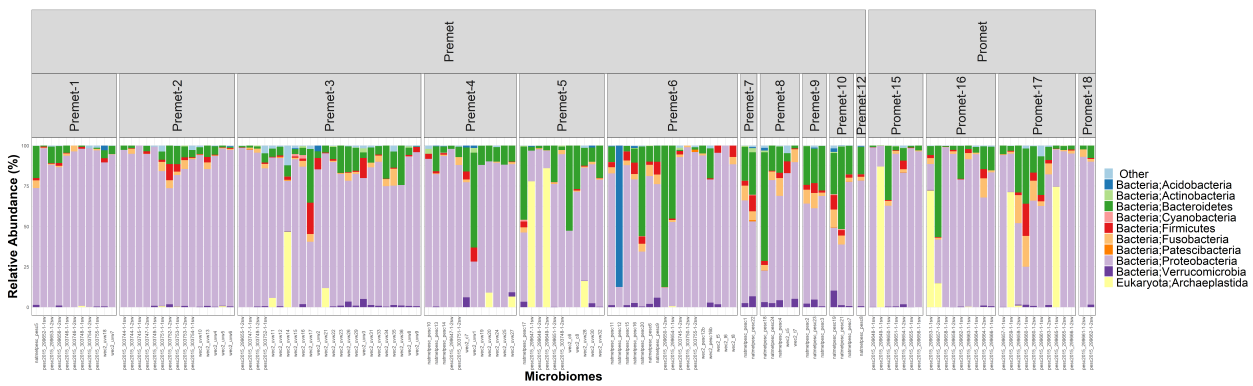


Figure 8: Relative phyla abundances of the tadpole microbiomes that was exposed to T3 and T4. The skin microbiomes (X-axis) of the tadpoles, classified according to their stage of development (bottom categories), are composed of 9 major phyla. No significant shifts in microbial communities occurred with tadpole development regardless of hormone exposure.

Clustering of Samples According to Sex

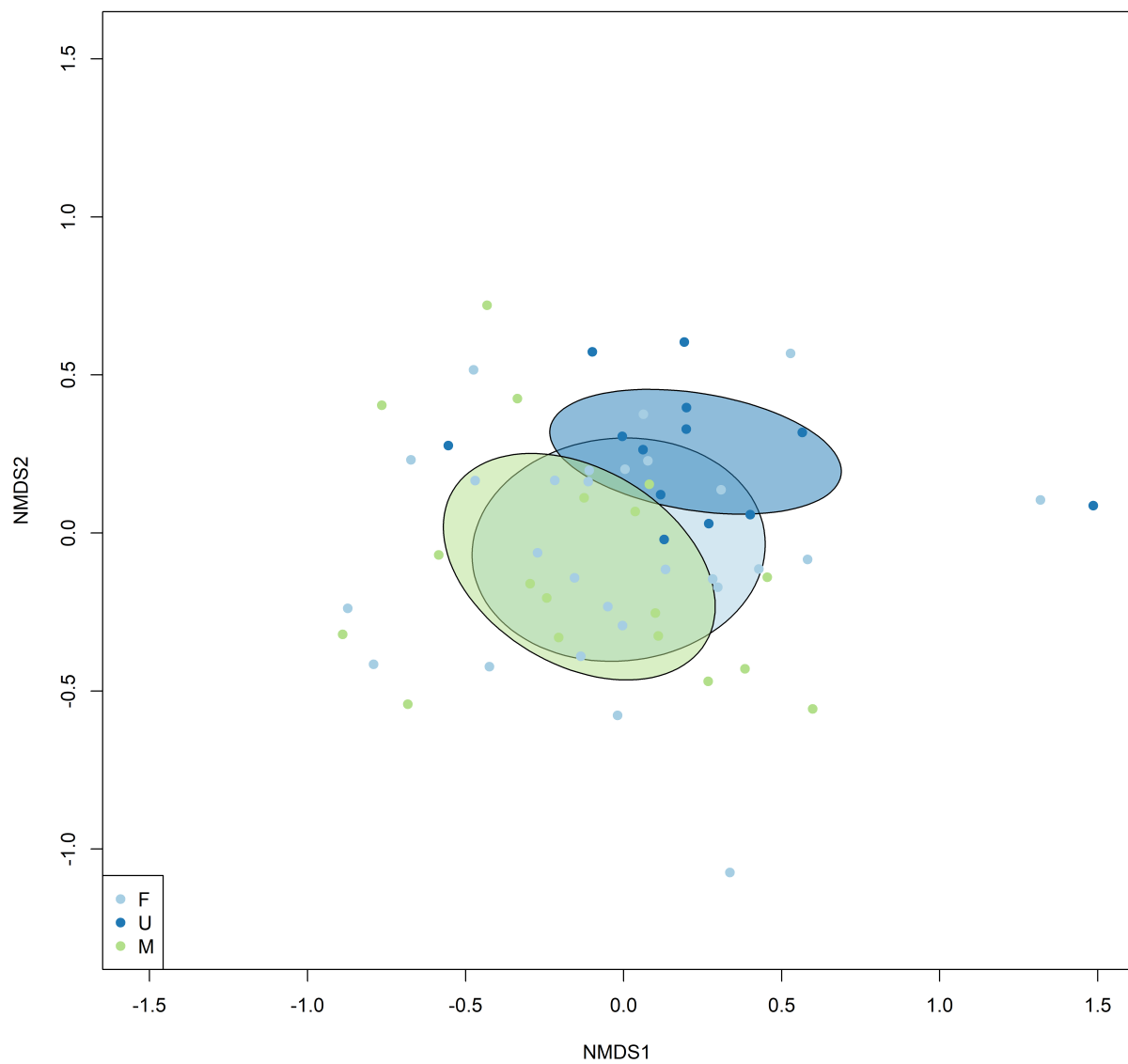


Figure 9: The sex of the frogs did not contribute to large changes in microbiome. The sex of the frog had no significant impact on the community composition.

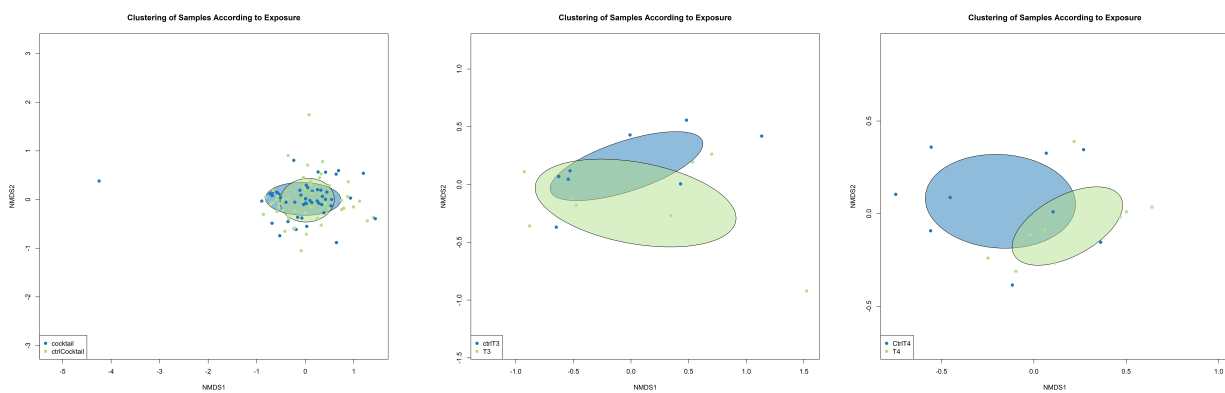


Figure 10: Clustering of microbiomes according to hormone exposure. There were no significant differences in the microbiomes of hormone exposed (green) versus control exposed (blue) as measured by the Bray-Curtis distance.

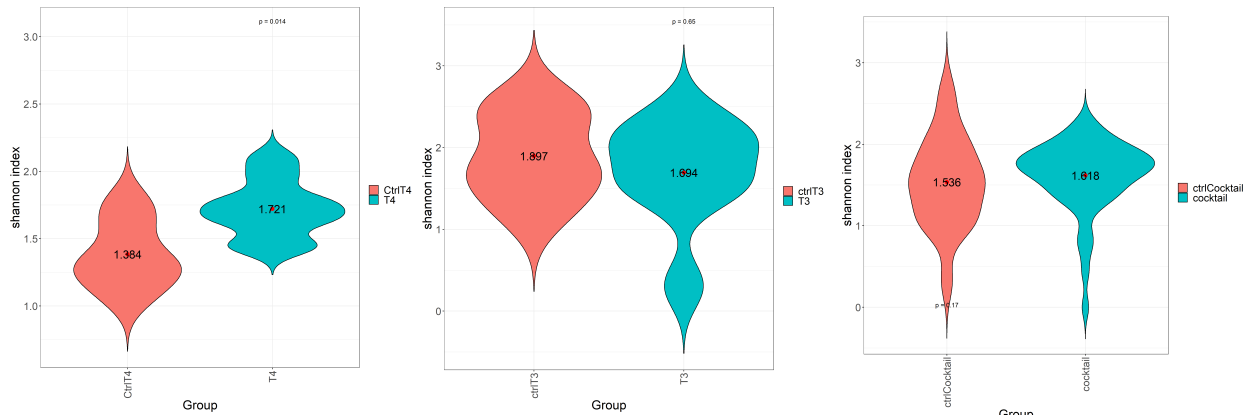


Figure 11: T4 exposure led to an increase in alpha diversity. Tadpoles exposed to T4 (cyan) exhibited a significant ($q=0.01$) increase in alpha diversity as measured by the Shannon Index compared to tadpoles (orange). T3 and E2 exposure did not have any effect on alpha diversity.

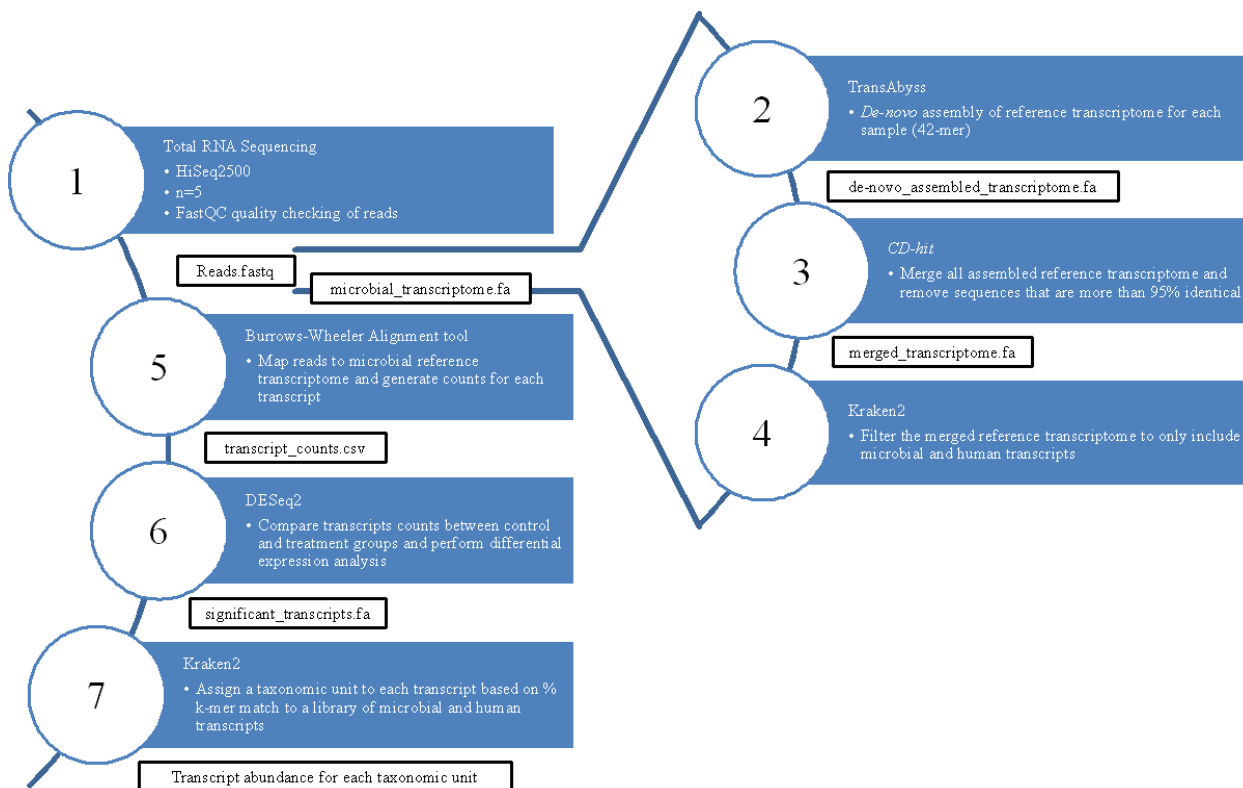


Figure 12: RNASeq methodology overview. figure description.

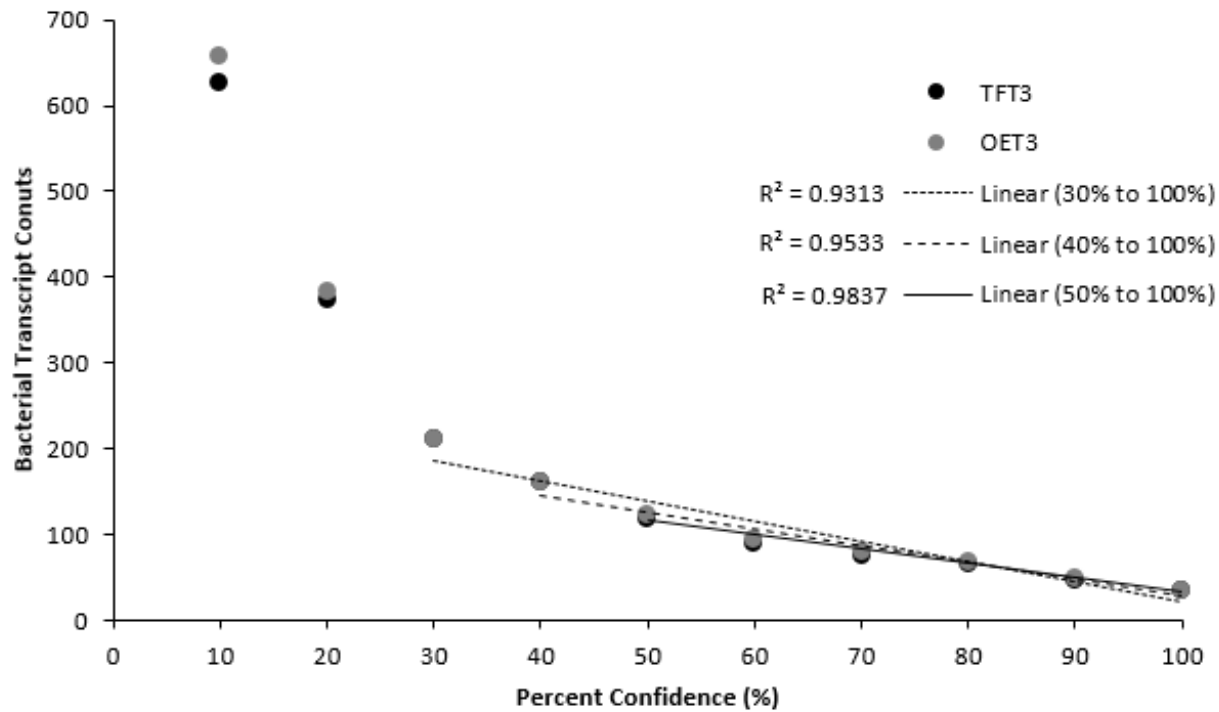


Figure 13: K-mer threshold for taxonomy identification. Excluding counts generated using a 10 to 30% confidence intervals for kraken2 mapping creates a linear correlation ($R^2 > 0.95$) between percent confidence and number of bacterial.

Figure 14: Relative Abundance of 16S Microbiomes at the Bacterial Phylum Level. The relative abundance of the top 10 bacterial phyla present across all samples represents >99% of all reads sequenced. The tadpole skin microbiome (labelled 1-23) consisted of predominately Proteobacteria (Purple). However, as life stage progresses, froglets are dominated by Verrucomicrobia. The relative distribution of phyla in the positive control (labelled POS) is as expected. Sterile swabs (labelled SSC) and negative controls (labelled NSC) have <2k reads on average.

Supplementary Information

References

- 1. Captive bottlenose dolphins and killer whales harbor a species-specific skin microbiota that varies among individuals**
M. Chiarello, S. Villéger, C. Bouvier, J. C. Auguet, T. Bouvier
Scientific Reports (2017-11-10) <https://doi.org/gck5k5>
DOI: [10.1038/s41598-017-15220-z](https://doi.org/10.1038/s41598-017-15220-z) · PMID: [29127421](#) · PMCID: [PMC5681658](#)
- 2. Onset and establishment of diazotrophs and other bacterial associates in the early life history stages of the coral *Acropora millepora***
Kimberley A. Lema, David G Bourne, Bette L. Willis
Molecular Ecology (2014-10) <https://doi.org/f6j683>
DOI: [10.1111/mec.12899](https://doi.org/10.1111/mec.12899) · PMID: [25156176](#)
- 3. Overfishing and nutrient pollution interact with temperature to disrupt coral reefs down to microbial scales**
Jesse R. Zaneveld, Deron E. Burkepile, Andrew A. Shantz, Catharine E. Pritchard, Ryan McMinds, Jérôme P. Payet, Rory Welsh, Adrienne M. S. Correa, Nathan P. Lemoine, Stephanie Rosales, ...
Rebecca Vega Thurber
Nature Communications (2016-06-07) <https://doi.org/ggc6g2>
DOI: [10.1038/ncomms11833](https://doi.org/10.1038/ncomms11833) · PMID: [27270557](#) · PMCID: [PMC4899628](#)
- 4. Biogeography of planktonic and coral-associated microorganisms across the Hawaiian Archipelago**
Jennifer L. Salerno, Brian W. Bowen, Michael S. Rappé
FEMS Microbiology Ecology (2016-08) <https://doi.org/f85c88>
DOI: [10.1093/femsec/fiw109](https://doi.org/10.1093/femsec/fiw109) · PMID: [27222221](#)
- 5. The microbiome extends to subepidermal compartments of normal skin**
Teruaki Nakatsuji, Hsin-I. Chiang, Shangi B. Jiang, Harish Nagarajan, Karsten Zengler, Richard L. Gallo
Nature Communications (2013-02-05) <https://doi.org/f4qxf>
DOI: [10.1038/ncomms2441](https://doi.org/10.1038/ncomms2441) · PMID: [23385576](#) · PMCID: [PMC3655727](#)
- 6. Skin microbiome promotes mast cell maturation by triggering stem cell factor production in keratinocytes**
Zhenping Wang, Nicholas Mascarenhas, Lars Eckmann, Yukiko Miyamoto, Xiaojun Sun, Toshiaki Kawakami, Anna Di Nardo
Journal of Allergy and Clinical Immunology (2017-04) <https://doi.org/f93jkh>
DOI: [10.1016/j.jaci.2016.09.019](https://doi.org/10.1016/j.jaci.2016.09.019) · PMID: [27746235](#) · PMCID: [PMC5385284](#)
- 7. Selective Antimicrobial Action Is Provided by Phenol-Soluble Modulins Derived from *Staphylococcus epidermidis*, a Normal Resident of the Skin**
Anna L. Cogen, Kenshi Yamasaki, Katheryn M. Sanchez, Robert A. Dorschner, Yuping Lai, Daniel T. MacLeod, Justin W. Torpey, Michael Otto, Victor Nizet, Judy E. Kim, Richard L. Gallo
Journal of Investigative Dermatology (2010-01) <https://doi.org/cpmx5t>
DOI: [10.1038/jid.2009.243](https://doi.org/10.1038/jid.2009.243) · PMID: [19710683](#) · PMCID: [PMC2796468](#)
- 8. The skin microbiome of vertebrates**
Ashley A. Ross, Aline Rodrigues Hoffmann, Josh D. Neufeld

Microbiome (2019-05-23) <https://doi.org/ghgh4h>
DOI: [10.1186/s40168-019-0694-6](https://doi.org/10.1186/s40168-019-0694-6) · PMID: [31122279](#) · PMCID: [PMC6533770](#)

9. The Human Oral Microbiome

Floyd E. Dewhirst, Tuste Chen, Jacques Izard, Bruce J. Paster, Anne C. R. Tanner, Wen-Han Yu, Abirami Lakshmanan, William G. Wade

Journal of Bacteriology (2010-10) <https://doi.org/czbkzv>

DOI: [10.1128/jb.00542-10](https://doi.org/10.1128/jb.00542-10) · PMID: [20656903](#) · PMCID: [PMC2944498](#)

10. Early gut colonizers shape parasite susceptibility and microbiota composition in honey bee workers

Ryan S. Schwarz, Nancy A. Moran, Jay D. Evans

Proceedings of the National Academy of Sciences (2016-08-16) <https://doi.org/f8zmpc>

DOI: [10.1073/pnas.1606631113](https://doi.org/10.1073/pnas.1606631113) · PMID: [27482088](#) · PMCID: [PMC4995961](#)

11. Microbiome Analysis Across a Natural Copper Gradient at a Proposed Northern Canadian Mine Site

Thea Van Rossum, Melanie M. Pylatuk, Heather L. Osachoff, Emma J. Griffiths, Raymond Lo, May Quach, Richard Palmer, Nicola Lower, Fiona S. L. Brinkman, Christopher J. Kennedy

Frontiers in Environmental Science (2016-01-06) <https://doi.org/gccwjv>

DOI: [10.3389/fenvs.2015.00084](https://doi.org/10.3389/fenvs.2015.00084)

12. Reproducible, interactive, scalable and extensible microbiome data science using QIIME 2

Evan Bolyen, Jai Ram Rideout, Matthew R. Dillon, Nicholas A. Bokulich, Christian C. Abnet, Gabriel A. Al-Ghalith, Harriet Alexander, Eric J. Alm, Manimozhiyan Arumugam, Francesco Asnicar, ... J. Gregory Caporaso

Nature Biotechnology (2019-07-24) <https://doi.org/gf5292>

DOI: [10.1038/s41587-019-0209-9](https://doi.org/10.1038/s41587-019-0209-9) · PMID: [31341288](#) · PMCID: [PMC7015180](#)

13. DADA2: High-resolution sample inference from Illumina amplicon data

Benjamin J Callahan, Paul J McMurdie, Michael J Rosen, Andrew W Han, Amy Jo A Johnson, Susan P Holmes

Nature Methods (2016-05-23) <https://doi.org/f84fxp>

DOI: [10.1038/nmeth.3869](https://doi.org/10.1038/nmeth.3869) · PMID: [27214047](#) · PMCID: [PMC4927377](#)

14. The SILVA ribosomal RNA gene database project: improved data processing and web-based tools

Christian Quast, Elmar Pruesse, Pelin Yilmaz, Jan Gerken, Timmy Schneemann, Pablo Yarza, Jörg Peplies, Frank Oliver Glöckner

Nucleic Acids Research (2012-11-27) <https://doi.org/gfb6mr>

DOI: [10.1093/nar/gks1219](https://doi.org/10.1093/nar/gks1219) · PMID: [23193283](#) · PMCID: [PMC3531112](#)

15. Respiratory Microbiome of Endangered Southern Resident Killer Whales and Microbiota of Surrounding Sea Surface Microlayer in the Eastern North Pacific

Stephen A. Raverty, Linda D. Rhodes, Erin Zabek, Azad Eshghi, Caroline E. Cameron, M. Bradley Hanson, J. Pete Schroeder

Scientific Reports (2017-03-24) <https://doi.org/f9z95d>

DOI: [10.1038/s41598-017-00457-5](https://doi.org/10.1038/s41598-017-00457-5) · PMID: [28341851](#) · PMCID: [PMC5428453](#)

16. Marine mammals harbor unique microbiotas shaped by and yet distinct from the sea

Elisabeth M. Bik, Elizabeth K. Costello, Alexandra D. Switzer, Benjamin J. Callahan, Susan P. Holmes, Randall S. Wells, Kevin P. Carlin, Eric D. Jensen, Stephanie Venn-Watson, David A. Relman

Nature Communications (2016-02-03) <https://doi.org/f8b9k7>
DOI: [10.1038/ncomms10516](https://doi.org/10.1038/ncomms10516) · PMID: [26839246](#) · PMCID: [PMC4742810](#)

17. **Micrococcus luteus - Survival in Amber**

C. L. Greenblatt, J. Baum, B. Y. Klein, S. Nachshon, V. Koltunov, R. J. Cano
Microbial Ecology (2004-05-28) <https://doi.org/dvc2jv>
DOI: [10.1007/s00248-003-2016-5](https://doi.org/10.1007/s00248-003-2016-5) · PMID: [15164240](#)

18. **Ecology of Viruses of Cold-Blooded Vertebrates**

V. GREGORY CHINCHAR
Elsevier BV (2000) <https://doi.org/bk6h2f>
DOI: [10.1016/b978-012362675-2/50012-4](https://doi.org/10.1016/b978-012362675-2/50012-4)